Proceedings of the 17th World Congress
The International Federation of Automatic Control
Seoul, Korea, July 6-11, 2008

Disturbance Rejection Control in Coordinated Systems ⋆

Keunmo Kang *, **David D. Zhang** *, **and Robert R. Bitmead** *

* *Department of Mechanical & Aerospace Engineering*
University of California San Diego
9500 Gilman Drive
La Jolla CA 92093-0411, USA
(Tel: 858-822-4940; e-mail: {kekang, dazhang, and rbitmead}@ucsd.edu)

Abstract: Coordinated system control with realistic disturbance is studied. We employ coordinated vehicles as an working problem. Vehicles attempt to keep a specified formation while avoiding collision in the presence of disturbance such as a wind gust. State estimators are used to estimate the self-states and the states of interacting vehicles via communication channels. Estimation performance is incorporated into control design and plays a central role in control performance. A numerical design approach is used to overcome limited knowledge about the disturbance and noises. A case study is given to demonstrate central ideas of the paper.

Keywords: disturbance rejection, coordinated system, cross-estimator, model predictive control

1. INTRODUCTION

Disturbance rejection is a standard purpose for the introduction of feedback control; without plant variability or disturbances, there might be little purpose in feedback. We study an approach to the incorporation of disturbance rejection in a coordinated control problem, where coordination is achieved by limited communication between systems and the imposition of constraints. The framework is easily understood in the context of coordinated multiple autonomous vehicles, where the state constraints are not to collide with the other vehicles and where communicated information is used by *cross-estimators* to estimate the other vehicles' states.

The focus of the work in this paper is on the formulation of a disturbance rejection controller starting from a disturbance description by data record alone to which is fitted an approximating state-space model, as opposed to commencing with an exact description by, say, a state-space, ARMA model, or bounded sets (Richards and How, 2004). In this way we hope to provide an approach suited to the rejection of realistic disturbances such as wind gusts on vehicles; deterministic disturbance cases were investigated in Francis and Wonham (1976). The contribution is, in the formulation of an estimator, to capture the predictable component of the disturbance and corresponding system behaviors well, and then to develop subsequently a mechanism to adjust the constraints in Model Predictive Control (MPC) to accommodate the estimator performance. Studies on coordination such as Richards and How (2004); Dunbar and Murray (2006); Kuwata and How (2006); Dunbar (2007) were proposed in a full-information-sharing environment. But our approach permits the inclusion of limited information sharing associated not only with the disturbance mentioned above but also with limited communication and measurement noises. A fairly complete example is provided using models of hovercraft and realistic wind gusts to demonstrate the approach and the achieved performance. The paper proceeds in several stages.

- formulation of estimators; 1) the self-state estimator of each vehicle's own state including its local disturbance state with driving signals due to the unpredictable disturbance and position measurement errors, 2) the cross-estimators of the states of other vehicles driven by their local signals plus communications errors.
- tuning estimator gains to predict the disturbance and the vehicles' behavior well, using methods akin to Adaptive Kalman Filtering (Haykin, 2001), and determination of the performance of the estimators; this performance is captured via the worst error bounds of the estimators.
- a case study using realistic disturbance signals and dynamic hovercraft models; incorporation of the worst error bounds into the determination of appropriate constraints for local MPC.

2. COORDINATED VEHICLE PROBLEM

Vehicles are to follow specified trajectories while attempting to keep a certain formation. Global formation information is given by some central authority and individual vehicle position offsets without disturbances would form a rigid-body-like formation. Some limited communication is permissible. Here we only consider the disturbance rejection on the local vehicle.

Consider a fleet of vehicles. We call the $i-$th vehicle in the fleet vehicle i. Its dynamic equation is given by

$$x^{i,v}_{k+1} = A_v x^{i,v}_k + B_v u^i_{k|k} + G_v q^{i,real}_k, \tag{1}$$

where $x^{i,v}_k$ is the state vector and $u^i_{k|k}$ denotes the MPC-input vector u^i_k computed at time k. We assume that the dynamics of each vehicle are linear, time-invariant, identical, and precisely given by A_v, B_v, and G_v. The disturbance $q^{i,real}_k$ is empirically measured from nature as time-domain-data sets before the

⋆ This research was supported by AFOSR Grant FA9550 – 05 – 1 – 0401.

estimator and control design processes and it is assumed that $q_k^{i,real}$ is the typical disturbance acting on vehicle i. We seek to describe $q_k^{i,real}$ by a linear model

$$\begin{aligned} x_{k+1}^{i,d} &= A_d^i x_k^{i,d} + G_d^i w_k^i, \\ q_k^i &= C_d^i x_k^{i,d}, \end{aligned} \tag{2}$$

with the disturbance state $x_k^{i,d}$, the output q_k^i (same dimension as $q_k^{i,real}$), and fictitious white noise input w_k^i. Since we will never obtain a perfect model for $q_k^{i,real}$, we only aim to obtain a reasonable model, where the acceptability of a model is determined by its ability to yield a good prediction of $q_k^{i,real}$. The model (2) is required to

- allow the construction of an observer-based predictor for $q_k^{i,real}$,
- preserve detectability (preferably observability) of the vehicle model

$$x_{k+1}^i = A^i x_k^i + B u_{k|k}^i + G^i w_k^i, \tag{3}$$

where

$$x_k^i = \begin{bmatrix} x_k^{i,v} \\ x_k^{i,d} \end{bmatrix}, A^i = \begin{bmatrix} A_v & G_v C_d^i \\ 0 & A_d^i \end{bmatrix}, B = \begin{bmatrix} B_v \\ 0 \end{bmatrix}, G^i = \begin{bmatrix} 0 \\ G_d^i \end{bmatrix},$$

$$\textit{position-output}: \; y_k^i = C x_k^{i,v},$$

$$\textit{measurement}: \; z_k^i = D x_k^{i,v} + v_k^i.$$

The measurement z_k^i is corrupted by bounded random noise v_k^i. Here we assume that the choice of A_d^i, G_d^i, and C_d^i satisfies the requirements. For clarity, we consider two vehicles (vehicle 1 and vehicle 2) and the formulation is given for vehicle 1. The design process for vehicle 2 is symmetric; and one can easily extend the formulation to include more vehicles.

We conclude this section by introducing some notations. For a vector x, $|x|$ denotes the euclidean norm of x. For a vector sequence x_k, $||x_k||_p \triangleq \max_k |x_k|$ is defined. For the state vector x_k^i, $\hat{x}_{k+j|k}^i$ is the estimation of x_{k+j}^i for the given measurements (z_k^i) up to time k and its error $x_{k+j}^i - \hat{x}_{k+j|k}^i$ is denoted by $\tilde{x}_{k+j|k}^i$. There will be superscripts and subscripts with superscripts meaning '*of*' and subscripts meaning '*at*'; for example, $\hat{x}_{i,k+j|k}^\ell$ ($z_{i,k}^\ell$) is the state estimate (measurement) *of* vehicle ℓ computed (taken) *at* (*by*) vehicle i. We will call $\hat{x}_{k+j|k}^i$ *self-estimates* and $\hat{x}_{i,k+j|k}^\ell$ *cross-estimates*.

3. SELF- AND CROSS-ESTIMATORS

The self-estimator of vehicle 1 is given by

$$\hat{x}_{k|k}^1 = (I - L^1 \bar{D}) A^1 \hat{x}_{k-1|k-1}^1 + (I - L^1 \bar{D}) B u_{k-1|k-1}^1 + L^1 z_k^1, \tag{4}$$

where $\bar{D} = [D \; 0]$ and L^1 is the self-estimator gain. Since $(A^1, \bar{D})$ is detectable there exists L^1 such that $(I - L^1 \bar{D}) A^1$ is stable. For cross-estimation, vehicle 1 receives the *full-state* information from vehicle 2 via a communication channel;

$$z_{1,k}^2 = \begin{bmatrix} \hat{x}_{k|k}^{2,v} + v_{1,k}^{2,v} \\ \hat{x}_{k|k}^{2,d} + v_{1,k}^{2,d} \end{bmatrix}.$$

The vectors $v_{1,k}^{2,v}$ and $v_{1,k}^{2,d}$ capture the bounded random communication noises such as quantization errors, packet dropout, and delay. Then the cross-estimator for vehicle 2 is

$$\hat{x}_{1,k+1|k}^2 = (A^2 - K_1^2) \hat{x}_{1,k|k-1}^2 + B u_{1,k|k-1}^2 + K_1^2 z_{1,k}^2, \tag{5}$$

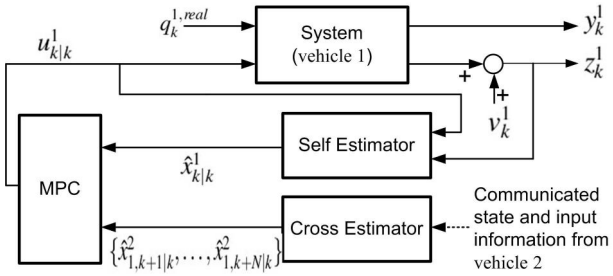

Fig. 1. The block diagram at vehicle 1. For cross-estimates computation, vehicle 1 receives the state and control information from vehicle 2. At the same time, vehicle 1 sends its state and control information to vehicle 2 (omitted in the figure).

where K_1^2 is the cross-estimator gain. There exists a stabilizing K_1^2 by the same argument as for the self-estimator case. For $j-$step ahead estimation, the input signal $u_{1,k+j-1|k-1}^2$ is also transmitted from vehicle 2 via the communication channel;

$$u_{1,k+j-1|k-1}^2 = u_{k+j-1|k-1}^2 + v_{1,k}^{2,j-1}, \; j = 1, 2, \ldots, N-1.$$

We also consider $v_{1,k}^{2,j-1}$ as bounded random communication noise. Note that the cross-estimator should have used $u_{1,k+j-1|k}^2$ for $j-$step ahead estimation at time k. But the control sequence at time k–1 is transmitted because $u_{k+j-1|k}^i$ is to be computed after the estimation process. The final control element is taken to be identical to $u_{k+N-2|k-1}^2$ since $u_{k+N-1|k-1}^2$ does not exist. The error by using the previous control is captured by

$$\begin{aligned} \eta_k^{2,j-1} &= u_{k+j-1|k}^2 - u_{k+j-1|k-1}^2, \; j = 1, \ldots, N-1, \\ \eta_k^{2,N-1} &= u_{k+N-1|k}^2 - u_{k+N-2|k-1}^2. \end{aligned} \tag{6}$$

The variability ($\eta_k^{2,j-1}$) is assumed to be bounded by the control constraint to appear later.

3.1 Control Requirement of Estimation

The local control at vehicle 1 has the following no-collision constraint to avoid collision with vehicle 2;

$$|\hat{y}_{k+j|k}^1 - \hat{y}_{1,k+j|k}^2| > \|\tilde{y}_{k+j|k}^1\|_p + \|\tilde{y}_{1,k+j|k}^2\|_p, \tag{7}$$

where $\tilde{y}_{k+j|k} \triangleq y_{k+j} - \hat{y}_{k+j|k}$. The constraint (7) means that the control must be chosen in such a way that the distance between $\hat{y}_{k+j|k}^1$ and $\hat{y}_{1,k+j|k}^2$ is greater than the sum of the worst position error bounds. This can be understood as no overlapping of two circles around $\hat{y}_{k+j|k}^1$ and $\hat{y}_{1,k+j|k}^2$ as shown in Fig. 2. One can also consider the size of the vehicles by adding an appropriate constant such as width of the vehicles. The right-hand-side of (7) can be fixed by $\|\tilde{y}_{k+1|k}^1\|_p + \|\tilde{y}_{1,k+1|k}^2\|_p$ since the vehicle is assured of receiving updated measurements before being required to assert constraint. Here we adopt this idea. The communication and estimation objective is to ensure that constraints are not always active. We want to have as small $\|\tilde{y}_{k+1|k}^1\|_p + \|\tilde{y}_{1,k+1|k}^2\|_p$ as possible so that the following condition is met:

$$\|\tilde{y}_{k+1|k}^1\|_p + \|\tilde{y}_{1,k+1|k}^2\|_p < d, \tag{9}$$

where d is the off-set between the vehicles as shown in Fig. 2. This is the minimum requirement for the estimators. Otherwise the no-collision constraint will be active even when $\hat{y}_{k+j|k}^1$ and $\hat{y}_{1.k+j|k}^2$ are at the target positions. This provides the key guideline for the estimator design.

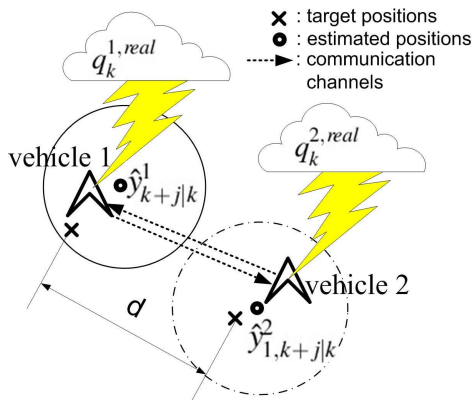

Fig. 2. The graphical description of the control at vehicle 1. The actual vehicle positions are inside the solid and dashed circles. Then $u^1_{k+j|k}$ steers $\hat{y}^1_{k+j|k}$ to its target position without overlapping the circles for all j=1,2,...,N to avoid collision.

3.2 Estimator Gain Tuning and Performance

The gain tuning begins with calculating $\tilde{y}^1_{k+1|k}$ and $\tilde{y}^2_{1,k+1|k}$ as shown in the following theorems.

Theorem 1. Suppose that vehicle i has the model (3) and a self-estimator as in (4). If $u^i_{k|k}$ is applied, then the input to output map $q^{i,real}_k$ and v^i_k to $\tilde{y}^i_{k+1|k}$ is given by

$$\begin{bmatrix}\tilde{x}^{i,v}_{k+1|k}\\ \hat{x}^{i,d}_{k+1|k}\end{bmatrix} = \begin{bmatrix}A_v - K^{i,1}D & -G_vC^i_d\\ K^{i,2}D & A^i_d\end{bmatrix}\begin{bmatrix}\tilde{x}^{i,v}_{k|k-1}\\ \hat{x}^{i,d}_{k|k-1}\end{bmatrix} + \begin{bmatrix}G_v\\ 0\end{bmatrix}q^{i,real}_k + \begin{bmatrix}-K^{i,1}\\ K^{i,2}\end{bmatrix}v^i_k, \qquad (10)$$
$$\tilde{y}^i_{k|k-1} = [C\ 0]\begin{bmatrix}\tilde{x}^{i,v}_{k|k-1}\\ \hat{x}^{i,d}_{k|k-1}\end{bmatrix},$$

where $K^i = A^iL^i = [K^{i,1^T}\ K^{i,2^T}]^T$.

Theorem 2. Suppose that vehicle ℓ has a model as in (3) and its cross-estimator at vehicle i as in (5). Then the input to output map from $q^{\ell,real}_k$, $\eta^{\ell,0}_k$, $v^{\ell,0}_{i,k}$, $v^{\ell,v}_{i,k}$, $v^{\ell,d}_{i,k}$, and v^ℓ_{k+1} to $\tilde{y}^\ell_{i,k+1|k}$ is given by (8) with

$$K^\ell_i = \begin{bmatrix}K^{\ell,11}_i & K^{\ell,12}_i\\ K^{\ell,21}_i & K^{\ell,22}_i\end{bmatrix},\ L^\ell = \begin{bmatrix}L^{\ell,1}\\ L^{\ell,2}\end{bmatrix}.$$

Denote $||\tilde{y}_{k+1|k}||_p$ evaluated for a single input e_k by $||\tilde{y}_{k+1|k}||^e_p$. Then the worst error bounds are given by

$$\begin{aligned}
\|\tilde{y}^1_{k+1|k}\|_p &= ||\tilde{y}^1_{k+1|k}||^{q^{1,real}}_p + ||\tilde{y}^1_{k+1|k}||^{v^1}_p,\\
\|\tilde{y}^2_{1,k+1|k}\|_p &= ||\tilde{y}^2_{1,k+1|k}||^{q^{2,real}}_p + ||\tilde{y}^2_{1,k+1|k}||^{\eta^{2,0}}_p\\
&\quad + ||\tilde{y}^2_{1,k+1|k}||^{v^{2,0}_1}_p + ||\tilde{y}^2_{1,k+1|k}||^{v^{2,v}_1}_p\\
&\quad + ||\tilde{y}^2_{1,k+1|k}||^{v^{2,d}_1}_p + ||\tilde{y}^2_{1,k+1|k}||^{v^2}_p.
\end{aligned} \qquad (11)$$

To compute $\|\tilde{y}^1_{k+1|k}\|_p$ and $\|\tilde{y}^2_{1,k+1|k}\|_p$, one may use peak-induced system norms ($\star$-norm) (Bu et al., 1996) of (10) and (8) for each input. This would be useful when the only knowledge about input is its bound. However since $q^{1,real}_k$ and $q^{2,real}_k$ are available as data records, $||\tilde{y}^1_{k+1|k}||^{q^{1,real}}_p$ and $||\tilde{y}^2_{1,k+1|k}||^{q^{2,real}}_p$ can be obtained by numerical simulation for given K^1 and K^2_1. This usually achieves less conservative $||\tilde{y}^1_{k+1|k}||^{q^{1,real}}_p$ and $||\tilde{y}^2_{1,k+1|k}||^{q^{2,real}}_p$ than computing them via peak-induced system norms. Since the rest of the inputs are bounded random sequences, for fixed K^1 and K^2_1, the remainder of $||\tilde{y}^1_{k+1|k}||_p$ and $||\tilde{y}^2_{1,k+1|k}||_p$ is calculated via peak-induced system norms.

Our aim is to design the estimators that achieve small $||\tilde{y}^1_{k+1|k}||_p$ and $||\tilde{y}^2_{1,k+1|k}||_p$. We may tune K^1 and K^2_1 directly by evaluating the difference in $||\tilde{y}^1_{k+1|k}||_p$ and $||\tilde{y}^2_{1,k+1|k}||_p$ with respect to variation in the elements of K^1 and K^2_1. However, if the dimension of the gains is high, this method would not be tractable. Furthermore it is hard to tune K^1 and K^2_1 only over the elements which are stabilizing. Alternatively since we can approximate the covariance matrix (R) of measurement and communication noises (denote R for self- and cross-estimators by R^1 and R^2_1 respectively), for fixed R^1 and R^2_1, one may use the Discrete time Algebraic Riccati Equation (DARE) to obtain stabilizing K^1 and K^2_1. In this case, one should pick Q^1 and Q^2_1 as the covariance matrices of the fictitious noise w_k in (3) for self- and cross-estimators. If we limit Q^1 and Q^2_1 to be symmetric positive semi-definite then it would be manageable to tune Q^1 and Q^2_1 by evaluating the difference in $\|\tilde{y}^1_{k+1|k}\|_p$ and $\|\tilde{y}^2_{1,k+1|k}\|_p$ with respect to variation in the elements of Q^1 and Q^2_1.

Gain Tuning and Performance Determination of Self-(Cross-) estimator

For fixed R^1 (R^2_1),

① *make an initial guess of* Q^1 (Q^2_1),

② *solve the DARE to obtain* K^1 (K^2_1),

③ *evaluate* $\|\tilde{y}^1_{k+1|k}\|_p$ ($\|\tilde{y}^2_{1,k+1|k}\|_p$),

④ *adjust elements of* Q^1 (Q^2_1) *and take the same procedure above (②∼③),*

⑤ *evaluate the difference in* $\|\tilde{y}^1_{k+1|k}\|_p$ ($\|\tilde{y}^2_{1,k+1|k}\|_p$) *to determine*

$$\begin{bmatrix}\tilde{x}^{\ell,v}_{i,k+1|k}\\ \hat{x}^{\ell,d}_{i,k+1|k}\\ \tilde{x}^{\ell,v}_{k+1|k+1}\\ \hat{x}^{\ell,d}_{k+1|k+1}\end{bmatrix} = \begin{bmatrix}A_v - K^{\ell,11}_i & K^{\ell,12}_i - G_vC^\ell_d & K^{\ell,11}_i & -K^{\ell,12}_i\\ K^{\ell,21}_i & A^\ell_d - K^{\ell,22}_i & -K^{\ell,21}_i & K^{\ell,22}_i\\ 0 & 0 & (I-L^{\ell,1}\bar{D})A_v & -(I-L^{\ell,1}\bar{D})G_vC^\ell_d\\ 0 & 0 & L^{\ell,2}\bar{D}A_v & A^\ell_d - L^{\ell,2}\bar{D}G_vC^\ell_d\end{bmatrix}\begin{bmatrix}\tilde{x}^{\ell,v}_{i,k|k-1}\\ \hat{x}^{\ell,d}_{i,k|k-1}\\ \tilde{x}^{\ell,v}_{k|k}\\ \hat{x}^{\ell,d}_{k|k}\end{bmatrix} + \begin{bmatrix}G_v\\ 0\\ (I-L^{\ell,1}\bar{D})G_v\\ L^{\ell,2}\bar{D}G_v\end{bmatrix}q^{\ell,real}_k$$
$$+ \begin{bmatrix}-B_v\\ 0\\ 0\end{bmatrix}\eta^{\ell,0}_k + \begin{bmatrix}-B_v\\ 0\\ 0\end{bmatrix}v^{\ell,0}_{i,k} + \begin{bmatrix}-K^{\ell,11}_i\\ K^{\ell,21}_i\\ 0\\ 0\end{bmatrix}v^{\ell,v}_{i,k} + \begin{bmatrix}-K^{\ell,12}_i\\ K^{\ell,22}_i\\ 0\\ 0\end{bmatrix}v^{\ell,d}_{i,k} + \begin{bmatrix}0\\ 0\\ -L^{\ell,1}\\ L^{\ell,2}\end{bmatrix}v^\ell_{k+1}, \quad \tilde{y}^\ell_{i,k|k-1} = [C\ 0\ 0\ 0]\begin{bmatrix}\tilde{x}^{\ell,v}_{i,k|k-1}\\ \hat{x}^{\ell,d}_{i,k|k-1}\\ \tilde{x}^{\ell,v}_{k|k}\\ \hat{x}^{\ell,d}_{k|k}\end{bmatrix}. \qquad (8)$$

the direction of steepest descent. Repeat (④∼⑤) until the descent is sufficiently small,
⑥ check if the final K^1 and K_1^2 satisfy (9). If so, move on to the control design. Otherwise use better measurement and communication systems or d must be increased.

Remarks:

- In Adaptive Kalman Filtering, gains are tuned on-line using sampled error covariance information. Here $\|\tilde{y}^1_{k+1|k}\|_p$ and $\|\tilde{y}^2_{1,k+1|k}\|_p$ information is used to adjust elements in Q^1 and Q_1^2 and, hence, tuning is performed off-line.
- To facilitate the deign process we proposed, one can use `fminsearch` in `matlab` that does not use analytic gradients.

4. CASE STUDY; FORMATION CONTROL

We demonstrate the incorporation of self- and cross-estimators into a two-vehicle-formation control problem as depicted in Fig. 3. Both vehicles are initially on their target positions. The

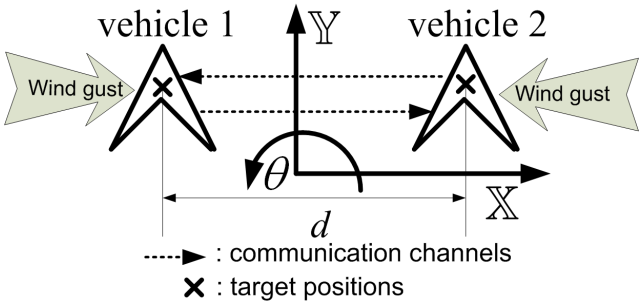

Fig. 3. A formation of two vehicles and the coordinates.

offset d is 0.6 m. To reveal the control performance effectively, we consider the following scenario:

- The gusts on vehicle 1 and 2 blow from the negative $\mathbb{X}$ and the positive $\mathbb{X}$ directions respectively with slight time delay,
- The vehicles' target positions are fixed all time. That is, their reference trajectories are constant.

One can implement more realistic wind gusts scenarios and consider time-varying reference trajectories easily. Typical and representative wind gusts are shown in Fig. 4. The control objective is to steer the vehicles to their target positions while avoiding collision in the presence of the disturbance.

4.1 Modeling

We create the discrete-time (0.3 sec sampling time) dynamical hovercraft model (1) based on HoTDeC (HOvercraft Testbed for DEcentralized Control, Rubel (2004)). The vehicle model has the state vector

$$x_k^{i,v} = \left[\mathbb{X}^i_{pk}\ \ \mathbb{Y}^i_{pk}\ \ \theta^i_{pk}\ \ \mathbb{X}^i_{sk}\ \ \mathbb{Y}^i_{sk}\ \ \theta^i_{sk}\right]^T.$$

The elements $\mathbb{X}^i_p$, $\mathbb{Y}^i_p$, $\mathbb{X}^i_s$, and $\mathbb{Y}^i_s$ represent positions and velocities in Cartesian coordinates respectively. The variables θ^i_p and θ^i_s are angular displacement and velocity of the vehicles respectively. Full-vehicle-state measurement is available. Three

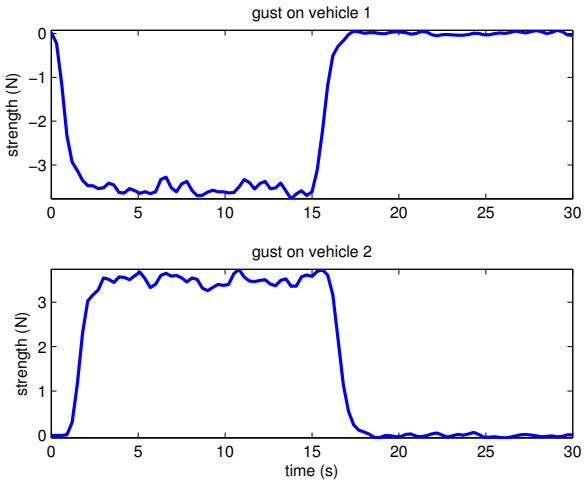

Fig. 4. The wind gust in thrust (N).

control inputs are available to control $\mathbb{X}$, $\mathbb{Y}$, and angular motions of the vehicle and have the limit defined by

$$\mathbb{U}^i \triangleq \{u \in \mathbb{R}^3 |\ |u|_\infty \le 5\},\ i = 1,2, \tag{12}$$

where $|\cdot|_\infty$ denotes the vector infinity norm. We model both disturbances in Fig. 4 as linear system models (2) with the disturbance state vector in $\mathbb{R}^4$. Then the combined vehicle models for vehicle 1 and 2 are constructed as (3). For computation, we assume that all the uncertainties are uniformly distributed. Their boundaries are

$$\begin{aligned} &|v^1_k|_\infty \le 0.01,\ |v^{2,j-1}_{1,k}|_\infty \le 0.001, \\ &|v^{2,v}_{1,k}|_\infty \le 0.001,\ \ |v^{2,d}_{1,k}|_\infty \le 0.001. \end{aligned} \tag{13}$$

We also assume that $\eta^{2,j}_k$ of (6) has the following limit

$$|\eta^{2,j}_k|_\infty \le 10,\ j = 0,1,2,\ldots,N-1. \tag{14}$$

The counterparts for vehicle 2 are the same.

4.2 Estimator Design and Performance

The self- and cross-estimators satisfying

$$\|\tilde{y}^1_{k+1|k}\|_p + \|\tilde{y}^2_{1,k+1|k}\|_p < d - 0.35 = 0.25 \tag{15}$$

are designed. Here we include the effect of vehicles' radii (2×0.175 m). After the tuning process, the achieved worst error bounds are

$$\|\tilde{y}^1_{k+1|k}\|_p = 0.038,\quad \|\tilde{y}^2_{1,k+1|k}\|_p = 0.167, \tag{16}$$

which satisfy the condition (15).

4.3 Incorporation into MPC

The proposed MPC for vehicle 1 is

$$\begin{aligned} \min_{\{u^1_{k|k},\ldots,u^1_{k+N-1|k}\}}\ & J^1_k = \sum_{j=0}^{N-1} (\hat{y}^1_{k+j+1|k} - r^1)^T Q_c (\hat{y}^1_{k+j+1|k} - r^1) \\ & + u^{1\,T}_{k+j|k} R_c u^1_{k+j|k}, \\ \textit{subject to}: \ & \hat{x}^1_{k+j+1|k} = A^1 \hat{x}^1_{k+j|k} + B u^1_{k+j|k}, \\ & \hat{y}^1_{k+j+1|k} = C \hat{x}^1_{k+j+1|k}, \\ & u^1_{k+j|k} \in \mathbb{U}^1, \\ & |\hat{y}^1_{k+j+1|k} - \hat{y}^2_{1,k+j+1|k}| > \|\tilde{y}^1_{k+1|k}\|_p + \|\tilde{y}^2_{1,k+1|k}\|_p + 0.35. \end{aligned}$$

Since the limit on $|\eta_k^{2,j}|_\infty$ is chosen to be 10 as in (14), we do not need additional control constraints other than $\mathbb{U}^1$ defined in (12).

Computationally the proposed MPC cannot be solved by standard quadratic programming due to non-convex nature of the no-collision constraint. We use a nonlinear optimization solver such as *SNOPT* (Gill et al., 2006) to compute a sub-optimal solution. The simulation is performed with the following parameters

$$N = 5, \;\; Q_c = 100 \times I, \;\; R_c = I, \qquad (17)$$

with appropriate dimensions of identity matrices I. In the next subsection, every figure but Fig. 6 will be given using (17).

4.4 Result and Discussion

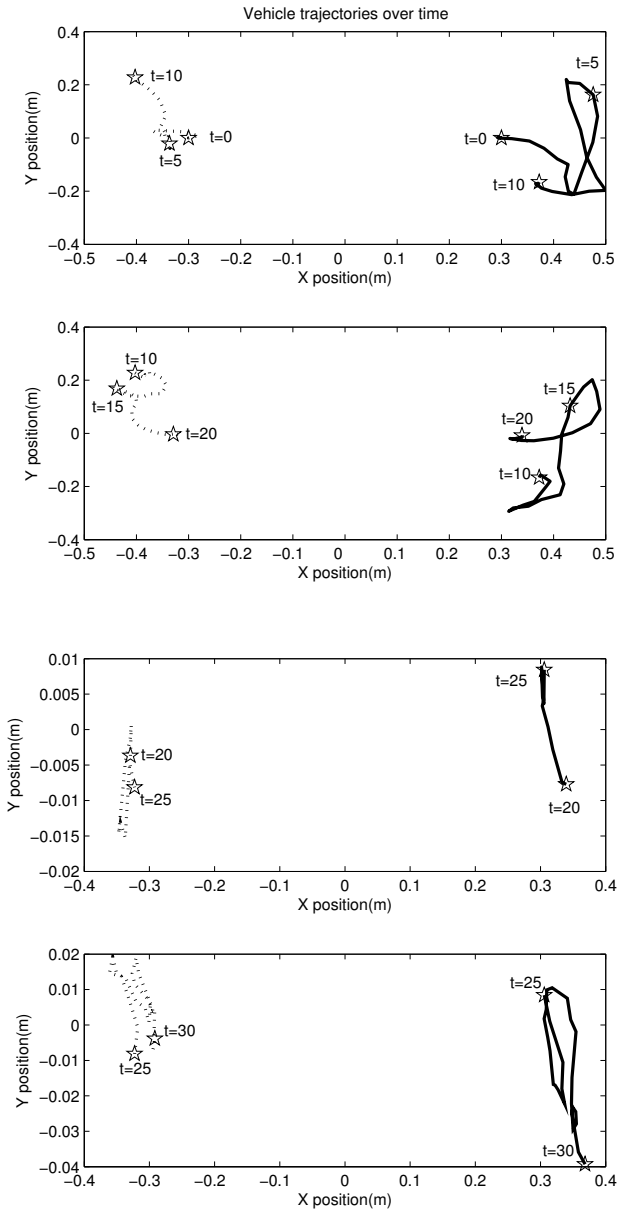

Fig. 5. Time trajectories of the vehicle 1 (solid lines) and vehicle 2 (dotted lines) with stared-time (t *sec*) marks.

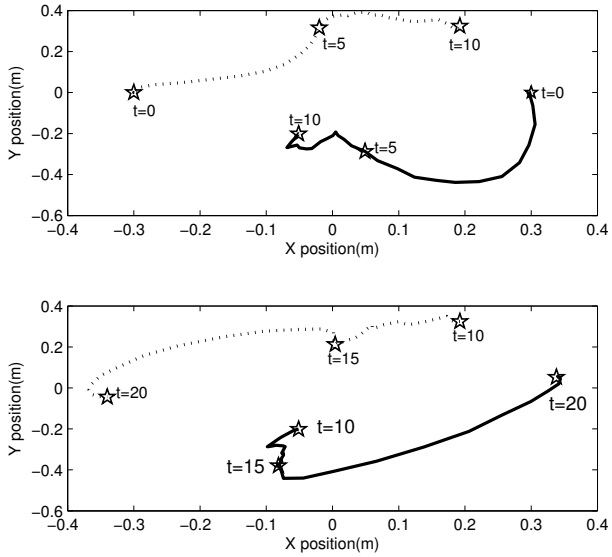

Fig. 6. Time trajectories of the vehicles using $Q_c = 25 \times I$ and $R_c = I$. Trajectories from 20 sec to 30 sec were omitted.

Entire vehicle trajectories with measurement and communication noises are depicted in Fig. 5. Due to the choice of Q_c and R_c in (17), their overall positions are not too far from their target positions; if smaller Q_c is used, for fixed R_c, the vehicles will make more dramatic moves to avoid collisions as shown in Fig. 6. In terms of activity of no-collision constraints, since there

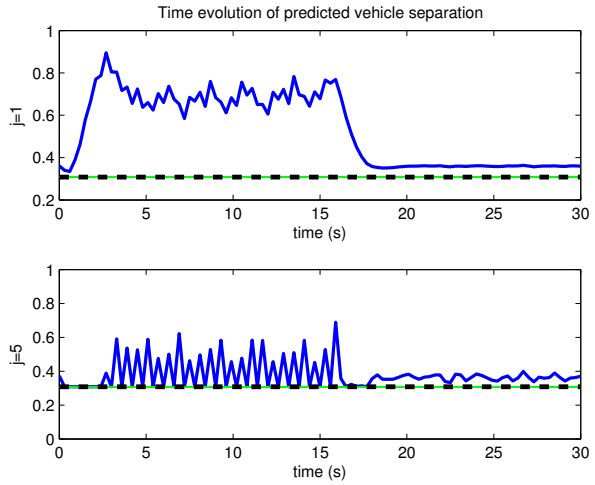

Fig. 7. Activity of one- and five-step ahead no-collision constraints without measurement and communication noises. The solid lines are the squared-expected distance between the vehicles for the computed input sequences. If the solid line touches the dashed line $[(\| \bar{y}^1_{k+1|k} \|_p + \| \bar{y}^2_{1,k+1|k} \|_p + 0.35)^2]$ at some moment, it means that the constraint was active at that time.

are no measurement and communication noises acting in Fig. 7, all active constraints are solely caused by the disturbance $q_k^{1,real}$ and $q_k^{2,real}$. On the other hand, when the measurement and communication noises (13) come into play, then the active constraints are caused by the combination of the disturbance and the noises. In particular, in the cross-prediction process, communicated inputs are corrupted by $v_{1,k}^{2,j-1}$ and the errors are

accumulated as prediction step j increases. As a result, more active constraints are observed as shown in Fig. 8. This leads to more conservative control overall as shown in Fig. 9; the more uncertainty the vehicles have, the more stand-off they need to avoid collision. In both cases, active constraints are not observed at one-step prediction stage especially when the wind gusts are active ($0 \sim 20sec$) due to the integral nature of the vehicle dynamics; extensive first-control-sequence energy is used to avoid constraint violations at the last prediction stage.

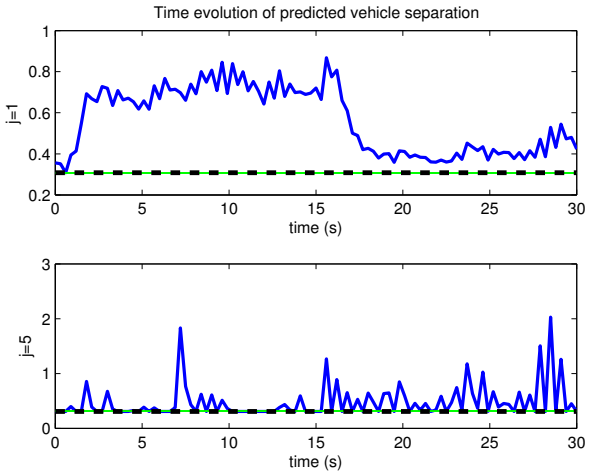

Fig. 8. Activity of one- and five-step ahead no-collision constraints when measurement and communication noises are acting.

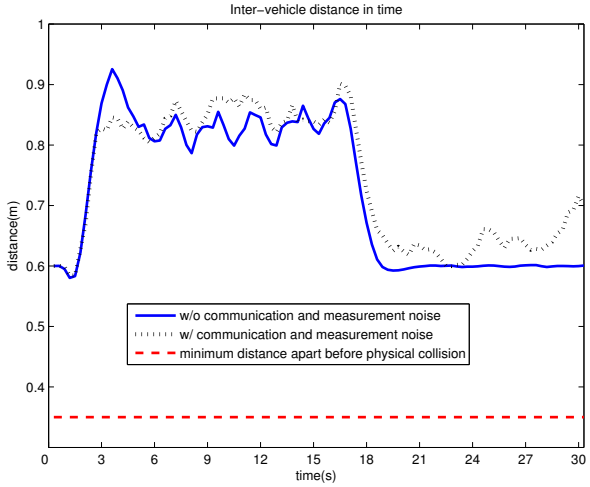

Fig. 9. Actual vehicle distance with and without measurement and communication noises. If the dotted or the solid line is below the dashed line, it means that collision occurred.

We observe that the actual distances between the vehicles are fairly above the minimum separation (0.35 m). It is because that computation of $\|\tilde{y}^1_{k+1|k}\|_p$ and $\|\tilde{y}^2_{1,k+1|k}\|_p$ involves peak-induced system norms which are usually conservative. This is more obvious in the cross-estimation part as shown in (16).

5. CONCLUSION AND FUTURE WORK

The disturbance rejection in coordinated systems can be effectively managed by the self- and cross-estimators and MPC. With the lack of knowledge about the disturbance and noise, numerical approach was proposed to obtain satisfactory estimation and control performance. Cross-estimator performance can be improved in the sense that more communication resources may lead to a smaller uncertainty region. Also, if the number of vehicles increases, limited communication resources of the vehicles matter and we need to manage the resources in an orderly manner not to harm control performance. Hence further analysis on the communication resources is necessary.

ACKNOWLEDGEMENTS

We gratefully acknowledge the instrumental support by professor Philip E. Gill at the UC San Diego Mathematics Department.

REFERENCES

J. Bu, M. Sznaier, and M. S. Holmes. A linear matrix inequality approach to systhesizing low order ℓ^1 controllers. *Proceedings of the 35th IEEE Conference on Decision and Control*, 1996.

W. B. Dunbar. Distributed receding horizon control of dynamically coupled nonlinear systems. *IEEE Transactions on Automatic Control*, 52:1249–1263, 2007.

W. B. Dunbar and R. M. Murray. Distributed receding horizon control for multi-vehicle formation stabilization. *Automatica*, 42:549–558, 2006.

B. A. Francis and W. M. Wonham. The internal model principle of control theory. *Automatica*, 12:457–465, 1976.

P. E. Gill, W. Murray, and M. A. Saunders. SNOPT Version 7. *http://cam.ucsd.edu/∼peg/*, 2006.

S. Haykin. *Adaptive Filter Theory*. Prentice Hall, 2001.

Y. Kuwata and J. How. Decentralized cooperative trajectory optimization for UAVs with coupling constraints. *Proceedings of the 45th IEEE Conference on Decision and Control*, 2006.

A. Richards and J. How. Decentralized model predictive control of cooperating UAVs. *Proceedings of the 43rd IEEE Conference on Decision and Control*, 2004.

J. Rubel. Master thesis : Design and control of hovercraft over a network. *University of Illinois Urbana-Champaign*, 2004.